Effects of wildfire on soil hydraulic properties on hillslopes in southwestern Oregon

by
Ryan Cole

A THESIS

submitted to

Oregon State University

University Honors College

in partial fulfillment of
the requirements for the
degree of

Honors Baccalaureate of Science in Natural Resources
(Honors Scholar)

Presented May 26, 2016
Commencement June 2016

AN ABSTRACT OF THE THESIS OF

Ryan Cole for the degree of Honors Baccalaureate of Science in Natural Resources presented on May 26, 2016. Title: Effects of wildfire on soil hydraulic properties on hillslopes in southwestern Oregon

Abstract approved: _____
Kevin D. Bladon

The purpose of this study was to investigate the effects of wildfire on soil hydraulic properties of forested hillslopes. The study site was located within the Stouts Creek wildfire, which burned approximately 10,705 ha of forest in southwestern Oregon in summer 2015. Three soil hydraulic properties (soil moisture, unsaturated hydraulic conductivity, and sorptivity) were measured along hillslope transects at 1 m, 5 m, and 10 m from the stream in burned and unburned catchments. Mean soil moisture in the burned hillslope was 1.2 – 1.5 times higher in the reference compared to the burned hillslope. Unsaturated hydraulic conductivity was approximately the same at the soil surface in the unburned and burned catchments, but conductivity at 10 cm depth in the soil was lower along the burned hillslope compared to the unburned hillslope. Sorptivity was lower at the soil surface, but unchanged at depth in the burned hillslope. A dye tracer experiment, to visually analyze subsurface flow in soil, was also conducted on burned and unburned hillslopes with highly variable results. Overall, results suggest the wildfire impacted soil structure at the surface, with likely impacts on surface runoff and subsurface flow.

Key Words: infiltration, hydrology, subsurface flow, soil moisture, hydraulic conductivity, water repellence, fire

Corresponding e-mail address: colery@oregonstate.edu

Effects of wildfire on soil hydraulic properties on hillslopes in southwestern Oregon

by
Ryan Cole

A THESIS

submitted to

Oregon State University

University Honors College

in partial fulfillment of
the requirements for the
degree of

Honors Baccalaureate of Science in Natural Resources
(Honors Scholar)

Presented May 26, 2016
Commencement June 2016

Honors Baccalaureate of Science in Natural Resources project of Ryan Cole presented on May 26, 2016.

APPROVED:

Kevin D. Bladon, Mentor, representing Department of Forest Engineering, Resources, and Management

Sharon Bywater-Reyes, Committee Member, representing Department of Forest Engineering, Resources, and Management

Ben Leshchinsky, Committee Member, representing Department of Forest Engineering, Resources, and Management

Toni Doolen, Dean, University Honors College

I understand that my project will become part of the permanent collection of Oregon State University, University Honors College. My signature below authorizes release of my project to any reader upon request.

Ryan Cole, Author

Acknowledgements

First of all, I'd like to thank Dr. Kevin Bladon for mentoring me through this abbreviated but arduous thesis-making process. You've helped me beyond learning about just hydrology but about this crazy scientific world in general. You have pushed me to ask interesting questions, to explore my interests, and feed my ever-growing curiosity about the natural world.

I'd like to thank Kira Puntenney for taking me under her wing with her Masters research. Working with you has been an eye opening experience, and I feel you've really tipped me in the right direction for my future endeavors.

I'd like to thank Noah Kanzig for the long hours he worked in the field to help me gather data. You've taken loads of weight off my shoulders (literally) and really helped keep our spirits up in the field.

Without the contributions of the following I would not have been able to complete this thesis: Karla Jarecke for her wealth of soil knowledge and her willingness to share that knowledge with me, Adrian Gallo for his knowledge and experience in hand soil texturing, Michael Bunn for his photo analysis and MATLAB abilities, and Sidney Post for his pivotal role in site selection access.

Finally, I'd like to thank Dr. Ben Leshchinsky and Dr. Sharon Bywater-Reyes for taking interest in this project, and their willingness to serve on my thesis committee.

1. Introduction

Wildfire is an important agent of natural disturbance in forested landscapes around the world (Bowman et al., 2009). Fires can dramatically alter ecosystems by returning vegetation communities to earlier seral stages, removing surficial organic soil horizons, increasing erosion rates, and reducing canopy cover (Roccaforte et al., 2012; Savage and Mast, 2005). Fire also affects the communities that rely on natural resources provided by forest ecosystems, that include timber production, clean water, and recreation opportunities (Emelko et al., 2011; Moritz et al., 2014). As populations increase, human society will put even greater strain on forest resources. Climate change will further compound the stress on forested ecosystems as changes in drought patterns and increases in temperature are expected to alter the global fire regime (Flannigan et al., 2013; Pechony and Shindell, 2010; Westerling et al., 2011). Increases in fire frequency and severity in western North America have already been observed (Westerling et al., 2006), a trend that is likely to continue in the future. Understanding fire effects on forested ecosystems is critical for land managers who must respond to resource scarcity as pressures increase on forest resources.

A valuable resource provided by headwater forests is water supply and water purification (Committee on Hydrologic Impacts of Forest Management, 2008). Estimates suggest that forests provide as much as $4.1 trillion USD in ecosystem services related to water filtration globally (Costanza et al., 1997). Replacing these ecosystem services with human infrastructure is a costly endeavor that must be undertaken after a large disturbance, such as a wildfire (Emelko et al., 2011; Smith et al., 2011). Many regions of the world, including the Pacific Northwest, have recently been identified as high-risk

areas for wildfire-induced impacts to water resources (Bladon et al., 2014; Robinne et al., 2016). In particular, wildfire can increase water temperature (Wagner et al., 2014), suspended sediment (Shakesby and Doerr, 2006), and chemical water quality parameters, such as phosphorus and nitrogen (Bladon et al., 2008; Emelko et al., 2016). Affected streams often exceed EPA mandated levels nitrate for safe drinking water (Rhoades et al., 2011). Wildfire can also affect the amount of water that reaches a stream, with evidence suggesting increases in total volume of runoff and peak flow after wildfire (Kunze and Stednick, 2006; Moody and Martin, 2001).

Changes in runoff are principally a result of wildfire impacts on soil physical (structure, aggregation, bulk density, particle size distribution) and hydrologic (hydraulic conductivity, infiltration, soil moisture) properties through intense heat and burning of surface organic horizons (Certini, 2005). However, wildfire effects on soil hydraulic properties are not well understood. There is little consensus on overall effects of fire, with some studies finding evidence of increases in soil moisture (Cardenas and Kanarek, 2014) while others see decreases after a fire (Ebel et al., 2012). There are also knowledge gaps in how wildfire affects the infiltration process in burned soils. Research suggests that infiltration decreases immediately after a wildfire, with multiple mechanisms proposed for this decrease (Ebel and Moody, 2013). Loss of soil organic horizons and vegetation can lead to decreased infiltration since organic materials often absorb more water than bare mineral soil (Wondzell and King, 2003). Surface sealing of pores by fine ash particles dislodged by rainfall can also lead to decreases in infiltration (DeBano, 2000; Wondzell and King, 2003). There is evidence of decreased infiltration related to hydrophobicity in burned soils creating a two-layer system – a wettable surface soil layer

and a water repellent layer just beneath the surface – that confines infiltration to shallow depths or macropores in non-repellent areas (Certini, 2005; Moody and Ebel, 2014; Nyman et al., 2010). Rates of infiltration are intimately related to antecedent soil moisture conditions. Hydraulic conductivity at low soil moistures (unsaturated) in burned soils may be near zero, while values of saturated hydraulic conductvity may be similar to unburned soils (Ebel and Moody, 2013). This is important when considering the real world application of water to a burned hillslope via rainfall. Rates of infiltration could follow a variety of different patterns as a function of time related to antecedent soil moisture and spatially variable soil hydraulic conductivity (Ebel and Moody, 2013).

Geomorphically, wildfires effects on soil properties can lower erosion thresholds leading to increased rates of runoff and surface erosion on forested hillslopes (Benavides-Solorio and MacDonald, 2001; Granged et al., 2011). This is well supported by previous research in the Pacific Northwest (Jackson and Roering, 2009; Wondzell and King, 2003). One of the primary reasons for post-fire increases in surface erosion and slope stability is changes in root reinforcement of the soil structure due to vegetation burning (Jackson and Roering, 2009). Wildfire can also lead to infiltration excess overland flow related to changes in soil water repellency or soil structure (Wondzell and King, 2003). Increases in overland flow and erosion could increase the amount of water and sediment reaching stream systems, thus affecting water quality and quantity (Silins et al., 2009; Stone et al., 2014). However, responses have been highly variable with the magnitude of post-fire erosion and sediment supply dependent on multiple factors, including sensitivity of the catchment to erosion, regional climate, geology, vegetation, and the wildfire regime (Martin and Moody, 2001; Robichaud, 2000). One of the fundamental difficulties

in predicting runoff and erosion following wildfire is due to incomplete knowledge regarding the linkage between soil hydraulic properties (e.g., hydraulic conductivity, sorptivity) that control infiltration across a range of burn severities and forest types (Moody et al., 2016).

Given the current gaps in knowledge and the importance of understanding factors contributing to post-fire runoff and erosion, the objectives of this study were to investigate changes in soil hydraulic properties. We conducted research within one of the largest, most severe fires of the 2015 fire season in southwestern Oregon (Stouts Creek fire) to investigate how fire alters soil hydraulic properties. In particular, the objectives were to investigate the effects of wildfire on infiltration and overland flow by measuring three soil hydraulic parameters (soil volumetric water content, unsaturated hydraulic conductivity, soil sorptivity). Spatial differences in hydraulic properties were investigated in relation to upslope distance from the stream. Finally, we also utilized rainfall simulations and dye tracing to investigate whether post-fire impacts on hydraulic properties influenced changes in overland and subsurface flow paths.

2. Methods

2.1. Site Description

The Stouts Creek wildfire burned approximately 10,695 ha of forestland along the foothills of the Cascade Mountains in southwestern Oregon from 30 July 2015 to 5 September 2015. Burn severity was spatially variable, with 17% of the landscape burning at high severity, 33% at medium severity, 28% at low severity, and 22% at very low severity, according to Burned Area Reflectance Classification (BARC) map (Figure 1).

Immediately prior to the fire, the region was in extreme drought condition, according to the US Drought Monitor – the low antecedent moisture conditions were ideal for rapid fire spread across the landscape and made containment difficult. As such, the fire spread quickly and unpredictably through the dry forest due to steep slopes and varying fuel densities. The burned area includes 25% private land, 21% Bureau of Land Management (BLM) land, and 54% U.S. Forest Service land.

Two small head headwater catchments (Stouts Creek and Callahan Creek) were selected for research, as they were more severely impacted by the Stouts Creek fire. Stouts Creek is a first- to fourth-order stream, whereas Callahan Creek is a first- to second-order stream. Both streams drain north to northeast into the South Umpqua River, which provides municipal water to many towns, including Canyonville and Roseburg, Oregon. The Stouts Creek watershed is owned and managed by the BLM and Roseburg Resources in a checkerboard pattern common in the western United States. The Callahan Creek watershed is managed by the US Forest Service as part of the Umpqua National Forest.

2.2. Soil surface hydraulic properties

Two hillslopes with similar characteristics in the Stouts Creek watershed were selected to investigate the effects of wildfire on the hydraulic properties of the local soils. One hillslope served as a reference site as it was located outside the perimeter of the Stouts Creek fire; the other hillslope (~2.5 km away) was burned at moderate to high severity by the Stouts Creek fire. The slope of the reference site was 69.0%, while the slope of the burned site was 69.5%. The reference site had a SSE facing aspect of 169

degrees, while the burned site had an ESE facing aspect of 112 degrees. The pre-fire soils on both sites were deep, well drained Sharpshooter loams formed from colluvium and residuum of quartz mica schist parent material according to NRCS soil survey data. The dominant tree species on both sites was Douglas-fir (*Pseudotsuga menziesii*), with patches of red alder (*Alnus rubra*) in the riparian areas.

Measurements of unsaturated hydraulic conductivity (K; L T^{-1}), sorptivity (S; L $T^{-1/2}$), and volumetric water content (θ; %) were collected from two depths (mineral soil surface and 10 cm) at five sites along each of three transects (1 m, 5 m, and 10 m from the stream) in both the reference and burned hillslopes. Points along each transect were located 5 m apart, such that they were independent. Thus, a total of 30 points were on each of the two hillslopes to compare soil hydraulic properties. The measurements of K and S were collected using a tension infiltrometer (Decagon Devices, 2.25 cm diameter Mini Disk) at an applied pressure head of -2 cm. At each site, surfaces were prepared by carefully removing the organic layer (if present) to expose the mineral soil surface of the soil. For samples at depth in the soil profile, the overlying soil was carefully removed producing a flat surface. A thin layer of sand was applied to the soil to ensure hydraulic contact with the tension infiltrometer. During measurements, the time of infiltration (seconds) and infiltration volume (ml) were recorded every 30 seconds until 15 ml had infiltrated or 12 minutes time had elapsed, whichever occurred first.

Measurements of cumulative infiltration and time were used to determine K based on the methods proposed by Zhang (1997), which uses the function:

$$I = C_1 t + C_2 \sqrt{t} \quad (1)$$

where I is the infiltration in cm, C_1 is a parameter related to hydraulic conductivity K (cm s^{-1}), C_2 is the soil sorptivity S (cm $s^{-1/2}$), and t is the time of infiltration (s). The hydraulic conductivity is calculated using the formula:

$$K = C_1/A \quad (2)$$

where C_1 is the hydraulic conductivity parameter from function (1), and A is the van Genuchten parameter for a given soil type – parameters were determined empirically for each soil type by Carsel and Parrish (1988). In this case, the van Genuchten parameter for the loam texture class (i.e., 6.27) was used. In cases where the infiltrometer trials returned negative hydraulic conductivity values (7 trials), these values were interpreted as near zero hydraulic conductivity. Negative infiltration is a physical impossibility, with such results likely due to due to the large amount of rocks near the surface or hydrophobicity, especially in the burned soil. In these cases, datasets were subset to include the greatest consecutive data string that resulted in a positive inflection on the polynomial regression. All of the hydraulic conductivity values given by the subset data remained lower than the positive infiltrometer trials, which is consistent with the assumption of flow restricting features or very low conductivity soils.

Prior to measurements of soil hydraulic properties, θ was measured using a DeltaT ML3 ThetaProbe soil moisture sensor and HH2 Meter (Delta-T Devices Ltd). The ML3 soil moisture probe uses electromagnetic waves at 100 MHz to measure the water content of soil and is accurate to ±1% volumetric moisture. Measurements were made by inserting the sensor horizontally into the soil profile, ensuring good contact between the rods and soil. In cases where there was strong resistance to insertion, the sensor was re-inserted in a new location.

Soil samples were also collected at each point from 0 to 5 cm of the soil depth, including the duff layer, and from 5 to 10 cm depth. Samples were stored in Whirl-pak bags for transport to the lab and placed in the freezer for storage until further analysis. Soil texture analysis was performed by hand texturing six of the soil samples in a lab to determine whether the burned soils remained the same texture indicated by the NRCS soil survey.

2.3. Dye experiment to assess infiltration and percolation

Two hillslopes in the Callahan Creek watershed were chosen to conduct an experiment using a dye tracer to investigate infiltration and sub-surface drainage. One unburned hillslope, downstream of the perimeter of the Stouts Creek fire, was used as a reference site. The burned hillslope was located < 1km upstream from the reference, within the high burn severity area. The slope of the reference site for the dye experiment was 64.0%; the slope of the burned site was 68.0%. The reference site had a NW facing aspect of 324 degrees, while the burned site had a WNW facing aspect of 282 degrees. The soils do not have an official taxonomic classification since the NRCS soil survey does not extend to these sites. The soil was hand textured to a sandy loam for both the reference and the burned site. The parent material is the same quartz mica schist as the Stouts Creek hillslopes.

Brilliant Blue FCF (CAS 3844-45-9) dye was used as a tracer to visually highlight infiltration and sub-surface flowpaths in the soil. Brilliant Blue FCF was chosen because of its low environmental toxicity, low sorption, high color contrast against the soil, and precedence of previous use in soil studies (Allaire et al., 2009). The methods used in this

study are adapted from those used by Weiler and Fluhler (2004) and Hardie et al. (2011). Brilliant Blue FCF dye (500g, powder) was spread by hand, ensuring even application, over 1 meter square plot on the soil surface for each trial. A rainfall simulator was used to simulate precipitation on the plot for 60 minutes at an intensity of 79 mm hr^{-1} on the reference plot and 90 mm hr^{-1} on the burned plot. Variability in rainfall intensity between the two plots was principally caused by wind affecting the rainfall patterns on the burned plot.

Following the rainfall simulation, the plots were covered with a tarp and left overnight for sub-surface drainage to continue. The following day, the plots were excavated and photographed to examine the flow pathways of dye in the soil. Three vertical soil faces were excavated in each of the burned and reference plots. These vertical soil faces were prepared using hand tools. The soil faces were cleaned and smoothed by hand to provide a flat vertical surface for accurate photography. Large rocks and roots made it difficult to create a smooth surface for some of the vertical faces, but care was taken to extract these features with minimal disturbance to the soil. After the excavation of each vertical face, multiple opaque tarps were hoisted over the plots to create a low light photography environment.

The camera (Nikon D7100) was set up on a tripod under the tarp cover at a distance of about 1.7 m from the plots. The distances for each image were chosen so that the camera was able to capture the entire soil face in one image. A scale bar and color card (X-Rite ColorChecker Classic Card) were included in each image to assist with image processing. Images of the dye stained faces were processed in Adobe Photoshop CS6 for color correction to separate the dye stained pixels from the unstained soil and

then in MATLAB to extract parameter-specific data. The threshold for classification of dye in the soil was qualitatively determined to be any pixel that had a cyan value greater than 206 in the CMY color space. Cyan values were chosen for thresholding because cyan was the color determined to be most distinctively different (opposite) of the principally red colored soils. We selected two parameters to describe the spatial distribution of dye staining: (a) the surface area density ($S_{V;}$ cm^{-1}) and (b) the volume density (V_V; %). The S_V is the stained surface area divided by the volume of the space, while the V_V is simply the fraction of pixels stained per depth.

2.4. Statistical Analysis

Statistical analysis of K, θ, and S were performed in R (R Core Team, 2014). Boxplots and histograms were created to visualize the distribution of the data. The Shapiro-Wilk test and Q-Q plots were used to further test the assumption that the data were normally distributed. While the tests suggested that the soil volumetric water content and S datasets were normally distributed, the hydraulic conductivity datasets did not meet this criteria. Thus, the soil volumetric water content and S datasets were analyzed using a 2 factor ANOVA to test the interaction between treatment (burned or unburned) and distance (1m, 5m, 10m) from stream. Attempts to normalize the unsaturated hydraulic conductivity with log transformations were unsuccessful. As such, the non-parametric Kruskal-Wallis test was used to assess the effects of treatment and distance from the stream on hydraulic conductivity in a series of single-factor tests.

3. Results

3.1 Soil moisture

Mean soil moisture in the surface soil layer (θ_{surf}; 0 – 5 cm) for all measurement points along the reference (unburned) hillslope was 20.4% ± 2.5% (Table 1). Alternatively, mean θ_{surf} for all measurement points on the burned hillslope was 13.9% ± 2.2%. Statistically, there was strong evidence that θ_{surf} was different between the burned and reference hillslopes (F = 11.8; p = .002). Mean soil moisture in the depth soil layer (θ_{depth}; 5 – 10 cm) for all measurement points on the reference hillslope was 22.0 ± 2.2% (Table 1). Mean θ_{depth} for all measurement points on the burned hillslope was 17.6 ± 2.8%. Statistically, there is mild evidence that θ_{depth} was different between the burned and reference hillslopes (F = 4.54; p = .042; Figure 3). Statistical comparisons between θ_{surf} and θ_{depth} in the reference site suggests no difference in moisture content (t = -0.83; p = .41). Similarly, there was no difference between θ_{surf} and θ_{depth} in the burned site (t = -1.85; p = .075). The distributions of θ_{surf} and θ_{depth} values are shown in Figure 2.

Mean θ_{surf} for the reference hillslope at measurement points a) 1 m from the stream was 17.3% ± 3.4%, b) 5 m from the stream was 20.2% ± 5.0%, and c) 10 m from the stream was 23.6 ± 6.2%. Comparatively, mean θ_{surf} for the burned hillslope at measurement points a) 1 m from the stream was 16.2% ± 5.1%, b) 5 m from the stream was 13.6% ± 5.2%, and c) 10 m from the stream was 11.9 ± 2.7%. The distribution of θ_{surf} values as a function of treatment and distance from stream is shown in Figure 3. Statistical analyses provided no evidence for differences in θ_{surf} as a function of distance from the stream in either the reference (F = 3.97; p = .068) or burned sites (F = 2.18; p =

.16). Therefore, the variability in θ_{surf} data appears to be most related to differences in site (burned vs. unburned) rather than distance from the stream.

Mean θ_{depth} for the reference hillslope at measurement points a) 1 m from the stream was 21.8 ± 6.6%, b) 5 m from the stream was 20.6 ± 2.8%, and c) 10 m from the stream was 23.4 ± 4.1%. Comparatively, mean θ_{depth} for the burned hillslope at measurement points a) 1 m from the stream was 18.9 ± 8.9%, b) 5 m from the stream was 18.5 ± 5.2%, and c) 10 m from the stream was 15.5 ± 2.9%. The distribution of θ_{depth} values as a function of treatment and distance from stream is presented in Figure 3. Statistical analyses provided no evidence for differences in θ_{depth} as a function of distance from the stream in either the reference (F = 0.31; p = .59) or burned sites (F = 0.75; p = .40). This suggests that the variation in θ_{depth} is only related to differences in site (burned vs. unburned).

3.2 Soil Unsaturated Hydraulic Conductivity

The median unsaturated hydraulic conductivity at the mineral soil surface (K_{surf}) for the reference hillslope was 3.34 mm hr^{-1} compared to 2.76 mm hr^{-1} for the burned hillslope (Table 2). Despite what appears to be much greater variability in K_{surf} in the burned sites (Figure 4), statistical analysis suggests there was no difference in in K_{surf} between the reference and burned sites (χ^2 = .073; p = .79). The median unsaturated hydraulic conductivity at 10 cm below the surface (K_{depth}) in the reference sites was 6.80 mm hr^{-1} compared to 2.32 mm hr^{-1} for the burned site (Figure 4; Table 2). The Kruskal-Wallis test provides statistical evidence that K_{depth} was different between the burned and unburned sites (χ^2 = 6.5; p = .01).

The relationship between K_{surf} and distance from stream was also investigated (Figure 5). Median K_{surf} in the unburned reference site was 2.95 mm hr^{-1} at 1 m from the stream, 3.93 mm hr^{-1} at 5 m from the stream, and 3.17 mm hr^{-1} at 10 m from the stream. Comparatively, median K_{surf} of the burned site was 6.47 mm hr^{-1} 1 m from the stream, 1.11 mm hr^{-1} at 5m from the stream, and 1.47 mm hr^{-1} at 10 m from the stream. Statistical analysis suggests there is no difference in in K_{surf} related to distance from the stream in the reference ($\chi^2 = 3.5$; $p = .17$) and the burned ($\chi^2 = 1.8$; $p = .40$) sites.

The relationship between K_{depth} and distance from stream was also investigated (Figure 5). Median K_{depth} along the reference hillslope was 10.6 mm hr^{-1} at 1 m from the stream, 6.36 mm hr^{-1} at 5 m from the stream, and 8.66 mm hr^{-1} 10 m from the stream. Median K_{depth} along the burned hillslope was 3.72 mm hr^{-1} at 1 m from the stream, 1.94 mm hr^{-1} at 5 m from the stream, and 6.02 mm hr^{-1} at 10 m from the stream. Statistical analysis suggests there was no difference in in K_{depth} related to distance from the stream in the reference ($\chi^2 = .18$; $p = .91$) and the burned ($\chi^2 = 1.2$; $p = .54$) sites.

The difference in unsaturated hydraulic conductivity between the surface and depth was compared between the reference and burned hillslopes by calculating a differential K (K_{diff}) from $K_{surf} - K_{depth}$ at each measurement point (Figure 6). A positive value of K_{diff} indicates K_{surf} was greater than K_{depth}, while a negative value indicates the opposite. In the unburned site, the vast majority (13 of 15, 87%) of trials indicated that unsaturated hydraulic conductivity was greater at depth than at the surface (median K_{diff}: -2.87 mm hr^{-1}, range: -19.30 mm hr^{-1} to 0.41 mm hr^{-1}). Alternatively, in the burned site, 8 of 15 trials (53%) indicated that unsaturated hydraulic conductivity was greater at the surface than at depth (median K_{diff}: 0.0699, range: -7.97 mm hr^{-1} to 5.41 mm hr^{-1}).

Statistical analysis suggests that K_{diff} was different between the burned and unburned sites ($\chi^2 = 5.9$; $p = .02$).

3.3 Soil Sorptivity

The overall mean sorptivity at the mineral soil surface (S_{surf}) from all measurement points in the reference site was 0.342 ± 0.073 mm $s^{-1/2}$ (Table 3). Alternatively, S_{surf} across all measurement points on the burned hillslope was 0.238 ± 0.030 mm $s^{-1/2}$ (Figure 7). ANOVA analysis suggested there was a difference in S_{surf} between the reference and burned sites ($F = 5.26$; $p = .029$). For comparison, mean sorptivity at 10 cm depth (S_{depth}) in the soil at the reference site was 0.234 ± 0.065 mm $s^{-1/2}$ compared to 0.326 ± 0.060 mm $s^{-1/2}$ for the burned site (Figure 7; Table 3). Statistical analysis suggests no difference in S_{depth} between the reference and burned sites ($F = 3.34$; $p = .078$).

Mean S_{surf} by distance from stream in the unburned site was 0.350 ± 0.197 mm $s^{-1/2}$ at 1 m from the stream, 0.375 ± 0.188 mm $s^{-1/2}$ at 5 m from the stream, and 0.298 ± 0.076 mm $s^{-1/2}$ at 10 m from the stream (Figure 8). In contrast, mean values in the burned site were 0.189 ± 0.044 mm $s^{-1/2}$ at 1 m from the stream, 0.215 ± 0.033 mm $s^{-1/2}$ at 5 m from the stream, and 0.309 ± 0.046 mm $s^{-1/2}$ at 10 m from the stream (Figure 8). ANOVA analysis suggests there is a difference in S_{surf} related to distance from the stream for the burned site ($F = 19.1$; $p < .001$), while there was no difference S_{surf} related to distance for the unburned site ($F = 0.281$; $p = .64$).

Mean S_{depth} by distance from stream in the unburned site were 0.317 ± 0.162 mm $s^{-1/2}$ at 1 m, 0.196 ± 0.140 mm $s^{-1/2}$ at 5 m, and 0.190 ± 0.086 mm $s^{-1/2}$ at 10 m from the

stream (Figure 8). Comparably, mean S_{depth} in the burned site were 0.288 ± 0.111 mm $s^{-1/2}$ at 1 m from the stream, 0.381 ± 0.184 mm $s^{-1/2}$ at 5 m from the stream, and 0.308 ± 0.058 mm $s^{-1/2}$ at 10 m from the stream (Figure 8). Statistical analysis suggests no difference S_{depth} related to distance from stream for the reference (F = 1.96; p = .18) or burned (F = 0.026; p = .87) sites.

3.4 Dye Experiment and Pattern Analysis

Despite high variability in infiltration and subsurface flow paths, image analysis of soil profiles along with qualitative information was indicative of differential flow responses between the reference plots (Figure 9) and burned plot (Figure 10). Across all soil profiles, the volume density (V_V), or fraction of soils stained with dye, appeared to be greater at depth in the burned site compared to the unburned site (Table 4). However, this was principally a result of the location of the soil profiles relative to the plot. Only one soil profile was excavated directly within each plot, with additional profiles at the downslope plot edge and 10 cm below the plot. Unfortunately, a large structural root and boulder running through the middle of the reference plot inhibited our ability to excavate additional faces at this site. As such, we performed similar excavations in the burned site to facilitate direct comparisons.

On the reference hillslope, soil profiles that were excavated 10 cm downslope of the hillslope (REF-10) and at the bottom edge of the 1 m^2 plot (REF0) had the lowest V_V of all of the plots. Comparatively, the only soil profile directly within the reference plot (REF+20) had the highest V_V throughout the soil profile, ranging from 95.8% to 98.1%

dye staining from 0 to 30 cm depth – this profile clearly had the most uniform wetting front from the surface to depth.

On the burned hillslope, a different pattern was evident in the soil profile excavated 10 cm downslope of the plot edge (BU-10), as it had consistently the highest V_V of the burned images, which extended from the surface to 40 cm depth. The soil profiles at the plot edge (BU0) and within the plot (BU+20) both show a high V_V for the first 10 – 15 cm depth before decreasing to 40 cm depth. Profiles BU0 and BU+20 both show significant overall decreases in V_V with depth compared to profile BU-10.

Differences in V_V between the burned and reference profiles highlight differences in subsurface flow between the two soils. The profile below the plot edge in the burned site (BU-10) had the greatest overall V_V relative to other burned profiles, compared to the reference site where the profile below the plot edge (REF-10) had the lowest V_V relative to the other reference profiles. This is evidence of greater subsurface lateral flow in the burned soils than the reference soils. Both profiles located within the plot area (BU+20 and REF+20) show V_V remaining higher over the top layers of soil, only decreasing significantly at 17 cm depth (BU+20) and 32 cm depth (REF+20). This is evidence that vertical dye flow through the soil matrix was greatest for the profiles located within the plot.

Trends in surface area density (S_V) display changes in the shape of flow paths and heterogeneity of flow at depth. Mean values of S_V are greater in the reference than the burned site across all depths (Table 4); however, there are distinctly different trends in S_V related to the distance of each profile from the plot edge. The general trend in S_V for the other five profiles was a minimum at the soil surface related to homogeneous flow across

the profile width, followed by a distinct increase in S_V over the first 10 – 20 cm depth. After this distinct increase, trends in S_V were variable, with three plots showing general decreases (BU0, REF0, REF-10) and two plots showing slight increases (BU+20, BU-10) with depth. Profile REF+20 was greatly affected by subsurface structural roots and boulders, leading it to display higher S_V at the surface that decreased initially with depth and then increased. Lower values of S_V in the burned site show that vertical subsurface flow paths were more coherent and homogeneous compared to the reference site.

In addition to the quantitative metrics V_V and S_V mentioned above, many observations of subsurface and overland flow were evident during rainfall simulation and excavation. In the unburned reference, there was significant amounts of vegetation covering the entire plot, while the unburned reference had a surface of mineral soil. This appeared to affect the infiltration and overland flow of the two plots. The reference plot had no visible overland flow during the rainfall simulation; all dye on the surface was contained within the plot area. In contrast, overland flow was visible within the first 5 minutes of rainfall in the burned plot, and continued throughout the entire simulation. Dye flow on the surface of the burned hillslope extended to a width of 1.658 m across the hillslope, wider than the 1 m plot. Overland dye flow extended 3.95 m below the bottom edge of the plot. Even this distance from the site of dye application, the width of the dye-stained soil was 0.485 m.

Also visible during the burned experiment was the creation of a small gully on the right side of the plot. This gully channeled the dye-stained overland flow for 4.13 m, starting 0.52 m from the top of the plot and extending to 3.95 m below the plot. The depth of the gully ranged from 1.0 cm deep at the bottom of the dye flow to 3.6 cm deep

at 2.0 m downslope of the start of the gully. During excavation this gully was visually related to concentrated subsurface flow evident on the right side of the soil profiles (Figure 10).

4. Discussion

4.1 Soil Hydraulic Properties

Soil moisture in the upper soil surface (θ_{surf}; 0-5 cm) on reference hillslopes was about 1.5-times greater than θ_{surf} on burned hillslopes at the end of the first rainy season following the Stouts Creek fire in southwestern Oregon. Similarly, soil moisture in a deeper soil layer (θ_{depth}) was also 1.2-times greater on the reference hillslope compared to the burned hillslope. A decrease in soil moisture, as observed in Stouts Creek, suggest that the fire likely impacted the soil structure and, therefore, soil hydraulic properties. Decreases in soil moisture in burned soils, particularly in the upper soil layers, have previously been attributed to increased evaporation due to greater exposure of soils to radiation, elevated absorption of radiation due to the dark color of ash and charcoal, and increased wind speeds and air temperatures at the soil surface (Ebel et al., 2012b; Holden et al., 2015; Soto and DiazFierros, 1997). Moreover, research following the 2010 Fourmile Canyon Fire near Boulder, CO in the Colorado Front Range, showed that drainage of near-surface (top 3 cm) soil water was more rapid on burned plots than unburned plots, resulting in more rapid declines in soil moisture (Ebel et al., 2012a). This effect was most pronounced on primarily south-facing slopes, similar to those in this study (Ebel et al., 2012a). However, it is important to note that observations of post-fire soil moisture have been contradictory, with many others observing wetter soils in burned

areas, principally due to reduced transpiration and canopy interception (Cardenas and Kanarek, 2014; Hatten et al., 2012).

The relationship between soil moisture and hydraulic conductivity (K) is a fundamental descriptor for the porous media flow properties of soils, with unique relationships for individual soil types based on soil physical properties (e.g., pore geometries) (Smith et al., 2002). As such, given the similar soil types between the reference and burned sites, these soils should have similar soil hydraulic relations (i.e., relationships between θ, K, and soil water potential (φ)). Typically, as soil moisture increases, the interconnectivity between pore spaces increases, resulting in less tortuous flow paths and increased unsaturated hydraulic conductivity (Smith et al., 2002). Under this assumption, K in the surface layer (K_{surf}) and at depth (K_{depth}) in the burned soil would both be expected to be substantially lower than in the reference hillslope as a result of lower soil moisture values (Figure 2). However, K_{surf} did not appear to be different between the reference and burned sites, suggesting that surface soil physical properties were impacted by the fire (Figure 4). Alternatively, at 10 cm depth the median K_{depth} was ~2.9-times greater in the reference site compared to the burned site, consistent with the assumptions related to lower θ in the burned site. As a result of the differential impacts at the surface and depth, the difference in unsaturated hydraulic conductivity between the surface and depth (K_{diff}) tended to be substantially lower in the reference site compared to the burned site. This is consistent with previous studies showing a two-layer system of infiltration in soils with a wettable surface soil layer over top of a hydrophobic subsurface layer that forms during combustion of soil organic matter during a fire (Certini, 2005; Moody and Ebel, 2014; Nyman et al., 2010). These observations are also consistent with

those of others that have observed that impacts to soil physical properties following moderate wildfire severity to be constrained to the upper 5 cm of soil (Litton and Santelices, 2003). However, it's important to note that others have observed that post-fire changes in soil structure and increases in bulk density lead to hydrophobicity and decreased infiltration and unsaturated hydraulic conductivity (DeBano, 2000; Wondzell and King, 2003). This, in part, may be due to the the moderate severity burn that impacted the hillslopes used to collect soil hydraulic properties, as compared to higher severity burns that others have observed (Ebel and Moody, 2013). Overall, the range of K observed at the surface and at depth following the Stouts Creek fire (Figure 4) are at the low end of the range of previous observations from the western U.S., which have observed K in fire affected soils between 10 to 100 mm hr^{-1} (Ebel et al., 2012b; Martin and Moody, 2001; Robichaud, 2000; Yates et al., 2000).

Changes in the characteristic soil hydraulic relations should also lead to differences in soil sorptivity (S) between the two sites. Since S is principally driven by capillary forces on water molecules in the soil matrix, and capillary forces are controlled by pore size and soil water potential (φ), changes in soil structure could have an effect on values of S. Laboratory experiments suggest that S is related to soil moisture (Moody et al., 2009), with minimum S coinciding with low (<2%) and high (>20%) soil moisture and maximum S between 3% and 8% soil moisture. Soil moisture values measured in the Stouts Creek sites are in the range of sorptivity values for which S decreases with increases in θ (Moody et al., 2009). As such, due to lower soil moisture in the burned sites (Figure 4), sorptivity would be expected to increase both at the surface and at 10 cm depth in the burned sites. The observed values suggest a different trend, with S_{surf} ~1.4

times higher in the reference compared to the burn, while S_{depth} a showed no difference between the two sites. As changes in S are not consistent with relationships to θ, this suggests wildfire had an effect on soil physical properties that control S (particle size distribution and soil water potential). Moreover, the decrease in S at the soil surface suggests that the infiltration regime is less influenced by capillary forces than before the fire, implying a change in pore sizes and soil-water potential relationships between the burned and reference hillslopes.

4.2 Dye tracing and subsurface flow

The soil dye tracing experiment provided additional evidence for impacts of wildfire on soil hydraulic properties, with influences on infiltration and sub-surface flow pathways. Dye image analysis and the volume density (V_V) suggested that within the reference plots, water infiltrated and moved vertically as a much more uniform wetting front than in the burned plot (Figure 9; REF+20). Moreover, the V_V from the soil profiles from the lower plot boundary (Figure 9; REF0) and below the plot (Figure 9; REF-10) were indicative of comparatively little lateral sub-surface flow in the reference plot compared to the burned plot. Lateral movement of water movement downslope in the reference site was principally via preferential flow paths, as indicated by the higher value of surface area density (S_V) deeper in these profiles. Alternatively, the burned plot showed much greater evidence of more heterogeneous finger flow both within and below the plot. Finger flow can be related to soil-water repellence or trapped air creating instability in the wetting front and typically occurs more often in dry soils (Hardie et al., 2011). Both the burned and reference profiles visually show evidence of finger flow, but

the fingers visible in the burned site were visually more defined with a lower S_V, which predominantly occurred in the sub-surface below a surface gully that formed during the simulation. In the burned plot, hydrophobicity and infiltration-excess overland flow was visually a dominant mechanism during the early portion of the rainfall simulation – this led to much greater downslope flow of water over the soil surface or in the near surface zone, resulting in erosion and gully formation. While infiltration-excess overland flow is rarely observed in forested environments, it has been recently observed in other environments following forest fires (Ebel et al., 2012b).

Such changes in runoff mechanisms due to impacts of fire on soil physical and hydraulic properties, and evidenced by this research, could lead to long-term changes in hillslope geomorphology and stream function. High severity wildfires can alter soil aggregation, structure, particle size distribution, bulk density and organic matter content by burning away organic cements that bind soil aggregates together and creating a fine ash layer (Certini, 2005). This generally results in soils that are less cohesive, more friable, and more erodible (Nyman et al., 2013; Shakesby and Doerr, 2006). Additionally, increased rain splash on the soil surface, and the creation of soil hydrophobicity, that decreases infiltration rates (DeBano, 2000) could also lead to increased post-fire erosion. There is evidence that erosion often increases after fire due to increased infiltration-excess overland flow that carries sediment down hillslopes (Gabet, 2003; Granged et al., 2011; Silins et al., 2009; Wondzell and King, 2003). However, others have suggested that the majority of sediment delivery to streams after wildfires may be due to increases in mass movements (Benavides-Solorio and MacDonald, 2001; Gabet and Bookter, 2008; Nyman et al., 2015), likely as a result of impacts to soil hydraulic properties.

Other studies using dye tracers (Hardie et al., 2011; Weiler and Fluhler, 2004) have calculated another metric, stained path width, for characterizing subsurface flow. This metric creates a quantitative parameter for analyzing the subsurface flowpaths beneath the soil. Stained path width can be used to determine the dominant type of flow based on analysis of the soil faces. Faces dominated with wide stained path widths show evidence of matrix flow, while narrow stained paths indicate macropore dominated flow (Weiler and Fluhler, 2004). Future analyses of soil profiles with dye tracers should include stained path width as a metric to more accurately characterize types of preferential flow.

An important knowledge gap that needs to be addressed in the future is the role of vegetation and organic soil horizons on the surface infiltration of forest soils. It is widely accepted that vegetation limits erosion and overland flow by protecting the soil surface from raindrop impact and adding structural stability to the soil surface through root cohesion (Wondzell and King, 2003; Certini, 2005, Shakesby et al., 2006). The rainfall simulation and dye experiment on the reference hillslope showed visual evidence of this, as the surface vegetation, especially moss, appeared to absorb large quantities of rainfall and prevent overland flow. Future investigations into infiltration into forest soils could attempt to isolate vegetative impacts on infiltration in order to create a much clearer understanding of wildfire effects on forest soils.

4.3 Spatial Heterogeneity

Values of sorptivity, hydraulic conductivity and soil moisture were all variable across the burned and unburned hillslopes. Variability in the datasets may have

obfuscated differences between burned and unburned soils. Only five points of data for each variable (S, K, θ) were collected for three distances from stream on each hillslope. The resulting sample size was small, which led to high variability for some parameters evident from the standard deviations in Table 1. Collecting more data may create less variable distributions, but variability of the datasets across the landscape is expected due to small scale changes in topography and soils.

Surprisingly, there were no spatial trends (distance from the stream) in soil moisture or unsaturated hydraulic conductivity in the burned or reference hillslopes. This was unexpected, as the assumption was that soils near the stream would be wetter than those further up the steep slopes (Famiglietti et al., 1998). It is possible that soils were moist from recent rains, which limited the differences between the upslope and riparian area soils. Variability in soil moisture was greater near the stream compared to the upslope at 10 cm depth (Figure 3). This was also unexpected, as it was assumed that the stream might act as a moderating influence on the differences between soil moisture readings. The high variability in soil moisture near the stream could be evidence of subsurface preferential flow into the stream, with some sections of streambank contributing different volumes of soil water to the stream than others.

Spatial heterogeneity of soil hydraulic properties could be related to heterogeneity of the fire. On hillslope scales wildfire is a highly spatially heterogeneous event (Figure 1). Burn severity can be influenced by vegetation type, initial moisture, topography, weather and fuel density, which are all highly variable across the landscape (Mermoz et al., 2005). Variability in burn severity and post-wildfire rainfall could lead to spatial heterogeneity in soil hydrophobicity (Blume et al., 2009). Spatial heterogeneity makes it

difficult to characterize the effects of wildfire on forest soils at a hillslope scale, suggesting smaller scale hydraulic properties control the movement of water from the time it infiltrates until it enters stream.

5. Conclusion

This study has found evidence of changes in soil properties at the soil surface, including soil moisture, unsaturated hydraulic conductivity, and sorptivity, immediately after the first wet season following a moderate to high severity wildfire. Effects of fire on soils resulted in lower soil moisture in the burned site compared to the unburned reference at the soil surface (0 – 5 cm) and at depth (5 – 10 cm). Hydraulic conductivity was not different at the soil surface but was lower at 10 cm depth. Soil sorptivity was also affected by the fire, with decreased soil sorptivity at the surface and no change in sorptivity at 10 cm depth.

Post-fire changes in soil hydraulic properties likely contributed to differential runoff mechanisms between burned and unburned sites. Dye tracing experiments indicated a more uniform wetting front at depth in the soil and relatively little lateral sub-surface flow in the reference sites. Alternatively, infiltration-excess overland flow, erosion, and preferential sub-surface flow (below gullies) was evident in the burned sites suggesting different runoff mechanisms. This could have implications on stream sediment levels and debris flows that affect the long-term geomorphology of the landscape.

While this study provided valuable preliminary insights into the potential effects of wildfire on soil hydraulic properties and subsurface flow, a more rigorous analysis of soil properties on burned hillslopes is necessary to strengthen the findings of this study.

Transect sizes and therefore datasets were limited during the survey of soil hydraulic properties. Increasing the size of the dataset of soil moisture and hydraulic properties through more field trials would strengthen relationships between the data. Replication of the dye experiment on more plots is also necessary to develop a clearer understanding of the effects of wildfire on the linkages between surface and subsurface flow processes. Future studies could build on the groundwork laid in this thesis to fill in knowledge gaps that remain about wildfire effects on forest soils.

6. References

Allaire, S.E., Roulier, S. and Cessna, A.J., 2009. Quantifying preferential flow in soils: A review of different techniques. Journal of Hydrology, 378(1-2): 179-204.

Benavides-Solorio, J. and MacDonald, L.H., 2001. Post-fire runoff and erosion from simulated rainfall on small plots, Colorado Front Range. Hydrological Processes, 15(15): 2931-2952.

Bladon, K.D., Emelko, M.B., Silins, U. and Stone, M., 2014. Wildfire and the future of water supply. Environmental Science & Technology, 48(16): 8936-8943.

Bladon, K.D., Silins, U., Wagner, M.J., Stone, M., Emelko, M.B., Mendoza, C.A., Devito, K.J. and Boon, S., 2008. Wildfire impacts on nitrogen concentration and production from headwater streams in southern Alberta's Rocky Mountains. Canadian Journal of Forest Research-Revue Canadienne De Recherche Forestiere, 38(9): 2359-2371.

Blume, T., Zehe, E. and Bronstert, A., 2009. Use of soil moisture dynamics and patterns at different spatio-temporal scales for the investigation of subsurface flow processes. Hydrology and Earth System Sciences, 13(7): 1215-1233.

Bowman, D.M.J.S., Balch, J.K., Artaxo, P., Bond, W.J., Carlson, J.M., Cochrane, M.A., D'Antonio, C.M., DeFries, R.S., Doyle, J.C., Harrison, S.P., Johnston, F.H., Keeley, J.E., Krawchuk, M.A., Kull, C.A., Marston, J.B., Moritz, M.A., Prentice, I.C., Roos, C.I., Scott, A.C., Swetnam, T.W., vanderWerf, G.R. and Pyne, S.J., 2009. Fire in the earth system. Science, 324(5926): 481-484.

Cardenas, M.B. and Kanarek, M.R., 2014. Soil moisture variation and dynamics across a wildfire burn boundary in a loblolly pine (*Pinus taeda*) forest. Journal of Hydrology, 519: 490–502.

Carsel, R.F. and Parrish, R.S., 1988. Developing joint probability-distributions of soil-water retention characteristics. Water Resources Research, 24(5): 755-769.

Certini, G., 2005. Effects of fire on properties of forest soils: a review. Oecologia, 143(1): 1-10.

Committee on Hydrologic Impacts of Forest Management, 2008. Hydrologic effects of a changing forest landscape: Report in brief, National Research Council, The National Academy of Sciences, Washington, D.C.

Costanza, R., d'Arge, R., de Groot, R., Farberk, S., Grasso, M., Hannon, B., Limburg, K., Naeem, S., O'Neill, R.V., Paruelo, J., Raskin, R.G., Suttonkk, P. and van den Belt, M., 1997. The value of the world's ecosystem services and natural capital. Nature, 387(6630): 253-260.

DeBano, L.F., 2000. The role of fire and soil heating on water repellency in wildland environments: a review. Journal of Hydrology, 231-232: 195-206.

Ebel, B.A., Hinckley, E.S. and Martin, D.A., 2012a. Soil-water dynamics and unsaturated storage during snowmelt following wildfire. Hydrology and Earth System Sciences, 16: 1401-1417.

Ebel, B.A. and Moody, J.A., 2013. Rethinking infiltration in wildfire-affected soils. Hydrological Processes, 27(10): 1510-1514.

Ebel, B.A., Moody, J.A. and Martin, D.A., 2012b. Hydrologic conditions controlling runoff generation immediately after wildfire. Water Resources Research, 48: W03529.

Emelko, M.B., Silins, U., Bladon, K.D. and Stone, M., 2011. Implications of land disturbance on drinking water treatability in a changing climate: Demonstrating the need for "source water supply and protection" strategies. Water Research, 45(2): 461-472.

Emelko, M.B., Stone, M., Silins, U., Allin, D., Collins, A.L., Williams, C.H.S., Martens, A.M. and Bladon, K.D., 2016. Sediment-phosphorus dynamics can shift aquatic ecology and cause downstream legacy effects after wildfire in large river systems. Global Change Biology, 22(3): 1168-1184.

Famiglietti, J.S., Rudnicki, J.W. and Rodell, M., 1998. Variability in surface moisture content along a hillslope transect: Rattlesnake Hill, Texas. Journal of Hydrology, 210: 259-281.

Flannigan, M., Cantin, A.S., de Groot, W.J., Wotton, M., Newbery, A. and Gowman, L.M., 2013. Global wildland fire season severity in the 21st century. Forest Ecology and Management, 294(S1): 54–61.

Gabet, E.J., 2003. Post-fire thin debris flows: Sediment transport and numerical modelling. Earth Surface Processes and Landforms, 28(12): 1341-1348.

Gabet, E.J. and Bookter, A., 2008. A morphometric analysis of gullies scoured by post-fire progressively bulked debris flows in southwest Montana, USA. Geomorphology, 96(3-4): 298-309.

Granged, A.J.P., Jordan, A., Zavala, L.M. and Barcenas, G., 2011. Fire-induced changes in soil water repellency increased fingered flow and runoff rates following the 2004 Huelva wildfire. Hydrological Processes, 25(10): 1614-1629.

Hardie, M.A., Cotching, W.E., Doyle, R.B., Holz, G., Lisson, S. and Mattern, K., 2011. Effect of antecedent soil moisture on preferential flow in a texture-contrast soil. Journal of Hydrology, 398(3-4): 191-201.

Hatten, J., Zabowski, D., Ogden, A., Theis, W. and Choi, B., 2012. Role of season and interval of prescribed burning on ponderosa pine growth in relation to soil inorganic N and P and moisture. Forest Ecology and Management, 269: 106-115.

Holden, S.R., Berhe, A.A. and Treseder, K.K., 2015. Decreases in soil moisture and organic matter quality suppress microbial decomposition following a boreal forest fire. Soil Biology & Biochemistry, 87: 1-9.

Jackson, M. and Roering, J.J., 2009. Post-fire geomorphic response in steep, forested landscapes: Oregon Coast Range, USA. Quaternary Science Reviews, 28(11-12): 1131-1146.

Kunze, M.D. and Stednick, J.D., 2006. Streamflow and suspended sediment yield following the 2000 Bobcat fire, Colorado. Hydrological Processes, 20(8): 1661-1681.

Litton, C.M. and Santelices, R., 2003. Effect of wildfire on soil physical and chemical properties in a *Nothofagus glauca* forest. Revista Chilena de Historia Natural, 76(4): 529-542.

Martin, D.A. and Moody, J.A., 2001. Comparison of soil infiltration rates in burned and unburned mountainous watersheds. Hydrological Processes, 15(15): 2893-2903.

Mermoz, M., Kitzberger, T. and Veblen, T.T., 2005. Landscape influences on occurrence and spread of wildfires in Patagonian forests and shrublands. Ecology, 86(10): 2707-2715.

Moody, J.A. and Ebel, B.A., 2014. Infiltration and runoff generation processes in fire-affected soils. Hydrological Processes, 28(9): 3432-3453.

Moody, J.A., Ebel, B.A., Nyman, P., Martin, D.A., Stoof, C. and McKinley, R., 2016. Relations between soil hydraulic properties and burn severity. International Journal of Wildland Fire, 25(3): 279-293.

Moody, J.A., Kinner, D.A. and Úbeda, X., 2009. Linking hydraulic properties of fire-affected soils to infiltration and water repellency. Journal of Hydrology, 379(3-4): 291-303.

Moody, J.A. and Martin, D.A., 2001. Post-fire rainfall intensity-peak discharge relations for three mountainous watersheds in the western USA. Hydrological Processes, 15(15): 2981-2993.

Moritz, M.A., Batllori, E., Bradstock, R.A., Gill, A.M., Handmer, J., Hessbur, P.F., Leonard, J., McCaffrey, S., Odion, D.C., Schoennagel, T. and Syphard, A.D., 2014. Learning to coexist with wildfire. Nature, 515: 58-66.

Nyman, P., Sheridan, G. and Lane, P.N.J., 2010. Synergistic effects of water repellency and macropore flow on the hydraulic conductivity of a burned forest soil, south-east Australia. Hydrological Processes, 24(20): 2871-2887.

Nyman, P., Sheridan, G.J., Moody, J.A., Smith, H.G., Noske, P.J. and Lane, P.N.J., 2013. Sediment availability on burned hillslopes. Journal of Geophysical Research-Earth Surface, 118(4): 2451-2467.

Nyman, P., Smith, H.G., Sherwin, C.B., Langhans, C., Lane, P.N.J. and Sheridan, G.J., 2015. Predicting sediment delivery from debris flows after wildfire. Geomorphology, 250: 173-186.

Pechony, O. and Shindell, D.T., 2010. Driving forces of global wildfires over the past millennium and the forthcoming century. Proceedings of the National Academy of Sciences of the United States of America, 107(45): 19167–19170.

R Core Team, 2014. R: A language and environment for statistical computing. R Foundation for Statistical Computing, Vienna, Austria.

Rhoades, C.C., Entwistle, D. and Butler, D., 2011. The influence of wildfire extent and severity on streamwater chemistry, sediment and temperature following the Hayman Fire, Colorado. International Journal of Wildland Fire, 20(3): 430-442.

Robichaud, P.R., 2000. Fire effects on infiltration rates after prescribed fire in Northern Rocky Mountain forests, USA. Journal of Hydrology, 231: 220-229.

Robinne, F.-N., Miller, C., Parisien, M.-A., Emelko, M.B., Bladon, K.D., Silins, U. and Flannigan, M., 2016. A global index for mapping the exposure of water resources to wildfire. Forests, 7(1): 22.

Roccaforte, J.P., Fulé, p.Z., Chancellor, W.W. and Laughlin, D.C., 2012. Woody debris and tree regeneration dynamics following severe wildfires in Arizona ponderosa pine forests. Canadian Journal of Forest Research, 42(3): 593-604.

Savage, M. and Mast, J.N., 2005. How resilient are southwestern ponderosa pine forests after crown fires? Canadian Journal of Forest Research, 35(4): 967-977.

Shakesby, R.A. and Doerr, S.H., 2006. Wildfire as a hydrological and geomorphological agent. Earth-Science Reviews, 74(3-4): 269-307.

Silins, U., Stone, M., Emelko, M.B. and Bladon, K.D., 2009. Sediment production following severe wildfire and post-fire salvage logging in the Rocky Mountain headwaters of the Oldman River Basin, Alberta. Catena, 38(3): 189-197.

Smith, H.G., Sheridan, G.J., Lane, P.N.J., Nyman, P. and Haydon, S., 2011. Wildfire effects on water quality in forest catchments: A review with implications for water supply. Journal of Hydrology, 396(1-2): 170-192.

Smith, R.E., Smettem, K.R.J., Broadbridge, P. and Woolhiser, D.A., 2002. Basic porous media hydraulics. In: R.E. Smith, K.R.J. Smettem, P. Broadbridge and D.A. Woolhiser (Editors), Infiltration Theory for Hydrologic Applications. American Geophysical Union, Washington, DC, pp. 7–23.

Soto, B. and DiazFierros, F., 1997. Soil water balance as affected by throughfall in gorse (Ulex europaeus, L) shrubland after burning. Journal of Hydrology, 195(1-4): 218-231.

Stone, M., Collins, A.L., Silins, U., Emelko, M.B. and Zhang, Y.S., 2014. The use of composite fingerprints to quantify sediment sources in a wildfire impacted landscape, Alberta, Canada. Science of the Total Environment, 473-474: 642-650.

Wagner, M.J., Bladon, K.D., Silins, U., Williams, C.H.S., Martens, A.M., Boon, S., MacDonald, R.J., Stone, M., Emelko, M.B. and Anderson, A., 2014. Catchment-scale stream temperature response to land disturbance by wildfire governed by surface-subsurface energy exchange and atmospheric controls. Journal of Hydrology, 517: 328–338.

Weiler, M. and Fluhler, H., 2004. Inferring flow types from dye patterns in macroporous soils. Geoderma, 120(1-2): 137-153.

Westerling, A.L., Hidalgo, H.G., Cayan, D.R. and Swetnam, T.W., 2006. Warming and earlier spring increase western U.S. forest wildfire activity. Science, 313(5789): 940-943.

Westerling, A.L., Turner, M.G., Smithwick, E.A.H., Romme, W.H. and Ryan, M.G., 2011. Continued warming could transform Greater Yellowstone fire regimes by mid-21st century. Proceedings of the National Academy of Sciences of the United States of America, 108(32): 13165-13170.

Wondzell, S.M. and King, J.G., 2003. Postfire erosional processes in the Pacific northwest and Rocky Mountain regions. Forest Ecology and Management, 178(1-2): 75-87.

Yates, D.N., Warner, T.T. and Leavesley, G.H., 2000. Prediction of a flash flood in complex terrain, Part II: a comparison of flood discharge simulations using rainfall input from radar, a dynamic model, and an automated algorithmic system. Journal of Applied Meteorology, 39: 815–825.

Zhang, R., 1997. Determination of soil sorptivity and hydraulic conductivity from the disk infiltrometer. Soil Science Society of America Journal, 61(4): 1024-1030.

Table 1: Means, medians, and standard deviations (SD) of soil moisture content (θ) in the upper soil surface (θ_{surf}; 0 – 5 cm) and at depth in the soil (θ_{depth}; 5 - 10 cm) arranged by treatment (reference and burn) and distance from stream (1 m, 5 m, 10 m).

	θ_{surf}			θ_{depth}		
	Mean	Median	SD	Mean	Median	SD
Reference	20.37%	20.30%	5.56%	21.95%	21.00%	4.79%
Burned	13.90%	13.50%	4.73%	17.63%	15.70%	6.20%
1 m Ref	17.26%	15.30%	3.57%	21.84%	21.00%	6.96%
1 m Burn	16.18%	16.90%	5.35%	18.88%	14.90%	9.31%
5 m Ref	20.24%	18.30%	5.25%	20.58%	20.70%	2.95%
5 m Burn	13.62%	13.50%	5.49%	18.48%	15.80%	5.49%
10 m Ref	23.62%	23.30%	6.52%	23.42%	22.20%	4.28%
10 m Burn	11.90%	12.10%	2.83%	15.54%	15.30%	3.05%

Table 2: Means, medians, and standard deviations (SD) of unsaturated hydraulic conductivity (K; mm hr^{-1}) at the soil surface (K_{surf}) and at 10 cm depth (K_{depth}) arranged by treatment (reference and burn) and distance from stream (1 m, 5 m, 10 m).

	K_{surf}			K_{depth}		
	Mean	Median	SD	Mean	Median	SD
Reference	3.46	3.34	1.92	8.78	6.80	5.49
Burned	4.03	2.76	3.91	4.51	2.32	5.53
1 m Ref	3.43	2.95	2.76	9.06	10.60	7.11
1 m Burn	5.13	6.47	2.27	3.12	3.72	2.48
5 m Ref	4.32	3.93	1.47	7.48	6.36	3.91
5 m Burn	2.32	1.11	2.60	2.68	1.94	2.78
10 m Ref	2.64	3.17	1.16	9.80	8.66	6.01
10 m Burn	4.64	1.47	6.00	7.74	6.02	8.57

Table 3: Means, medians, and standard deviations (SD) of soil sorptivity (*S;* mm $s^{-1/2}$) at the surface (S_{surf}) and at 10 cm depth (S_{depth}) arranged by treatment (reference and burn) and distance from stream (1 m, 5 m, 10 m).

	S_{surf}			S_{depth}		
	Mean	Median	SD	Mean	Median	SD
Reference	0.0342	0.0322	0.0162	0.0234	0.0208	0.0143
Burned	0.0238	0.0229	0.0067	0.0326	0.0313	0.0131
1 m Ref	0.0350	0.0407	0.0206	0.0317	0.0385	0.0171
1 m Burn	0.0189	0.0213	0.0047	0.0288	0.0296	0.0117
5 m Ref	0.0375	0.0348	0.0197	0.0196	0.0201	0.0147
5 m Burn	0.0215	0.0228	0.0035	0.0381	0.0285	0.0193
10 m Ref	0.0298	0.0276	0.0079	0.0190	0.0207	0.0090
10 m Burn	0.0309	0.0314	0.0049	0.0308	0.0328	0.0061

Table 4: Means and standard deviations (SD) of volume density (V_V, %) and surface area density (S_V, cm^{-1}) for four depth classes in soil profiles (0 – 10 cm, 10 – 20 cm, 20 – 30 cm, 30 – 40 cm) arranged by treatment

	Reference				Burned			
	V_V		S_V		V_V		S_V	
Depth	Mean	SD	Mean	SD	Mean	SD	Mean	SD
0-10cm	93.80	5.4	0.94	0.52	89.23	9.1	0.92	0.63
10-20cm	69.66	23.3	1.75	1.05	79.74	9.5	1.50	0.62
20-30cm	55.62	30.0	1.71	0.81	65.56	12.7	1.43	0.70
30-40cm	44.00	27.2	1.90	0.72	56.37	11.0	1.50	0.64

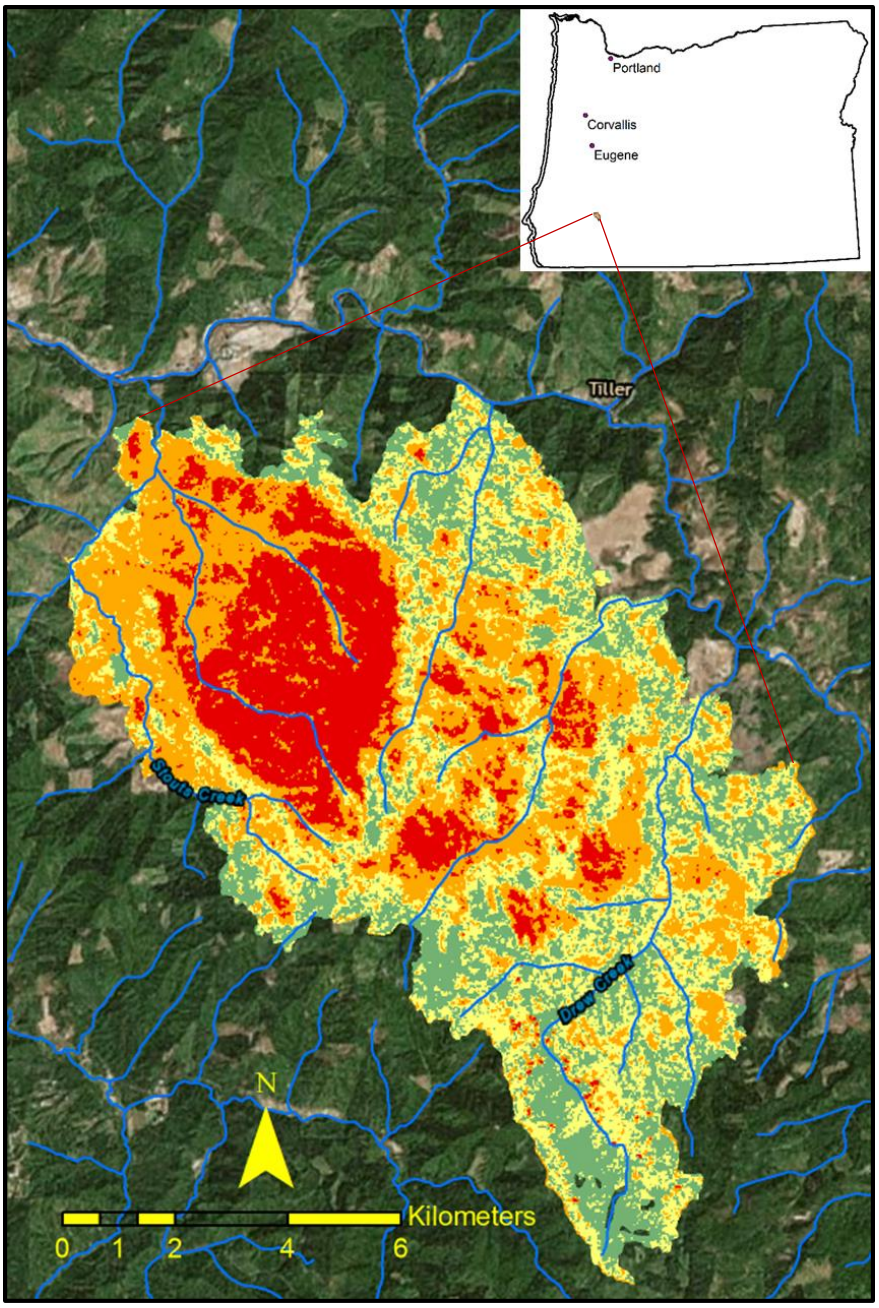

Figure 1: Burned Area Reflectance Classification (BARC) map of the Stouts Creek wildfire area in southwestern Oregon (green = unburned; yellow = low burn severity, orange = moderate burn severity, red = high burn severity).

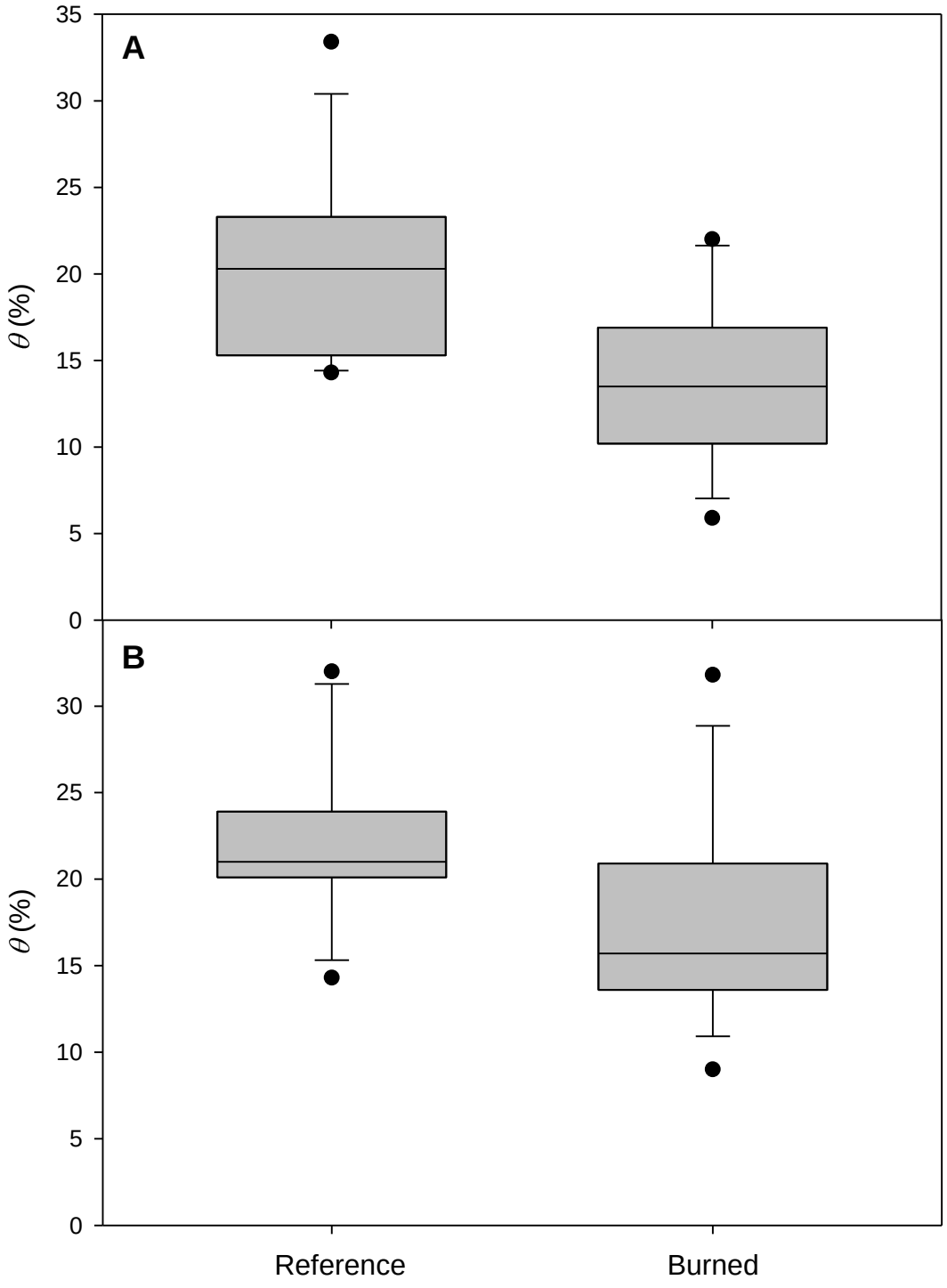

Figure 2: Soil moisture in the A) surface soil layer (θ_{surf}; 0 – 5 cm) and B) depth soil layer (θ_{depth}; 5 – 10 cm) for all measurement points along the reference (unburned) hillslope and on the burned hillslope.

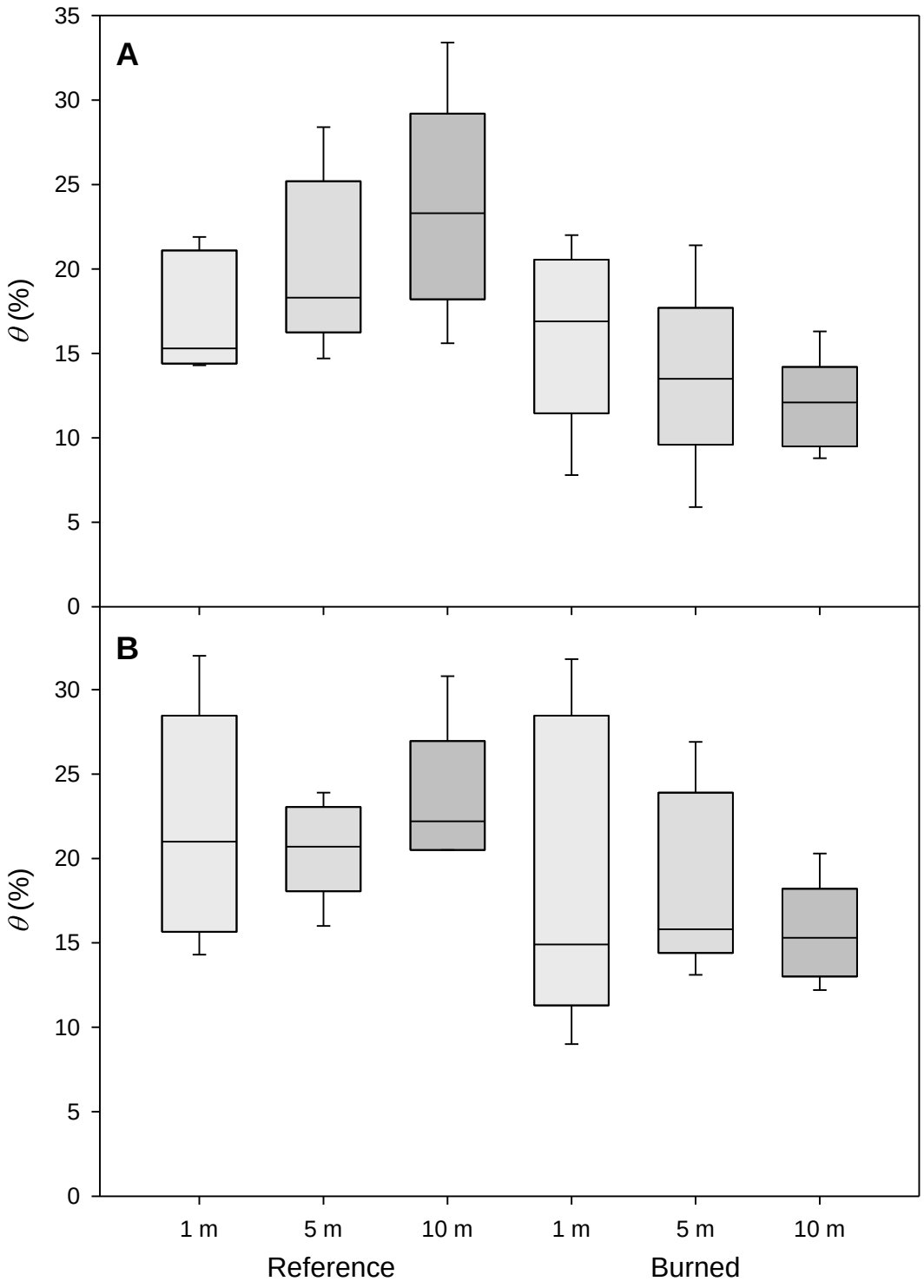

Figure 3: Soil moisture in the A) surface soil layer (θ_{surf}; 0 – 5 cm) and B) depth soil layer (θ_{depth}; 5 – 10 cm) at three distances (1 m, 5 m, 10 m) from the stream edge in the reference (unburned) and burned hillslope.

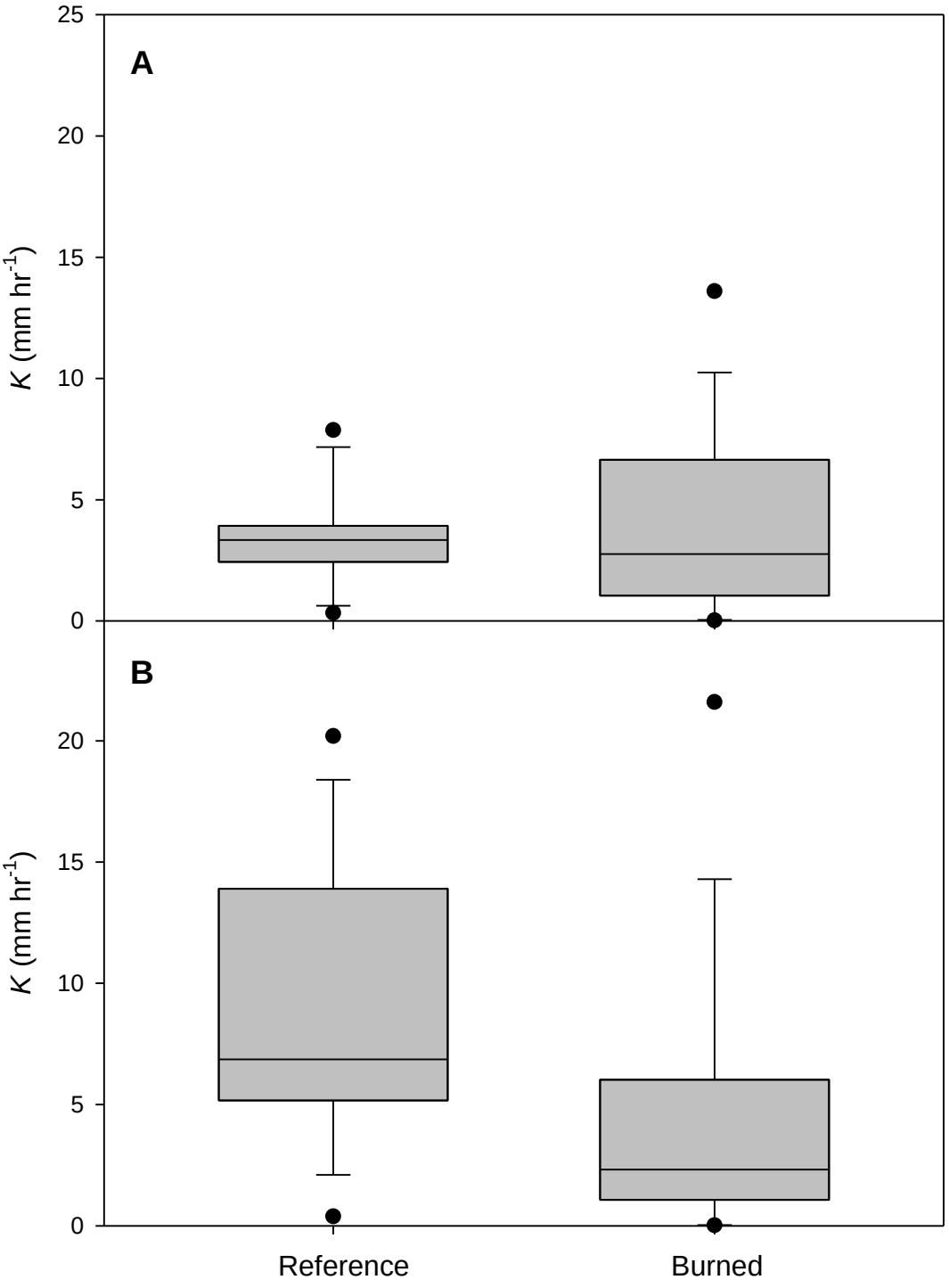

Figure 4: Hydraulic conductivity at A) the soil surface (K_{surf}) and B) at 10 cm depth in the soil (K_{depth}) for all measurement points along the reference (unburned) hillslope and on the burned hillslope.

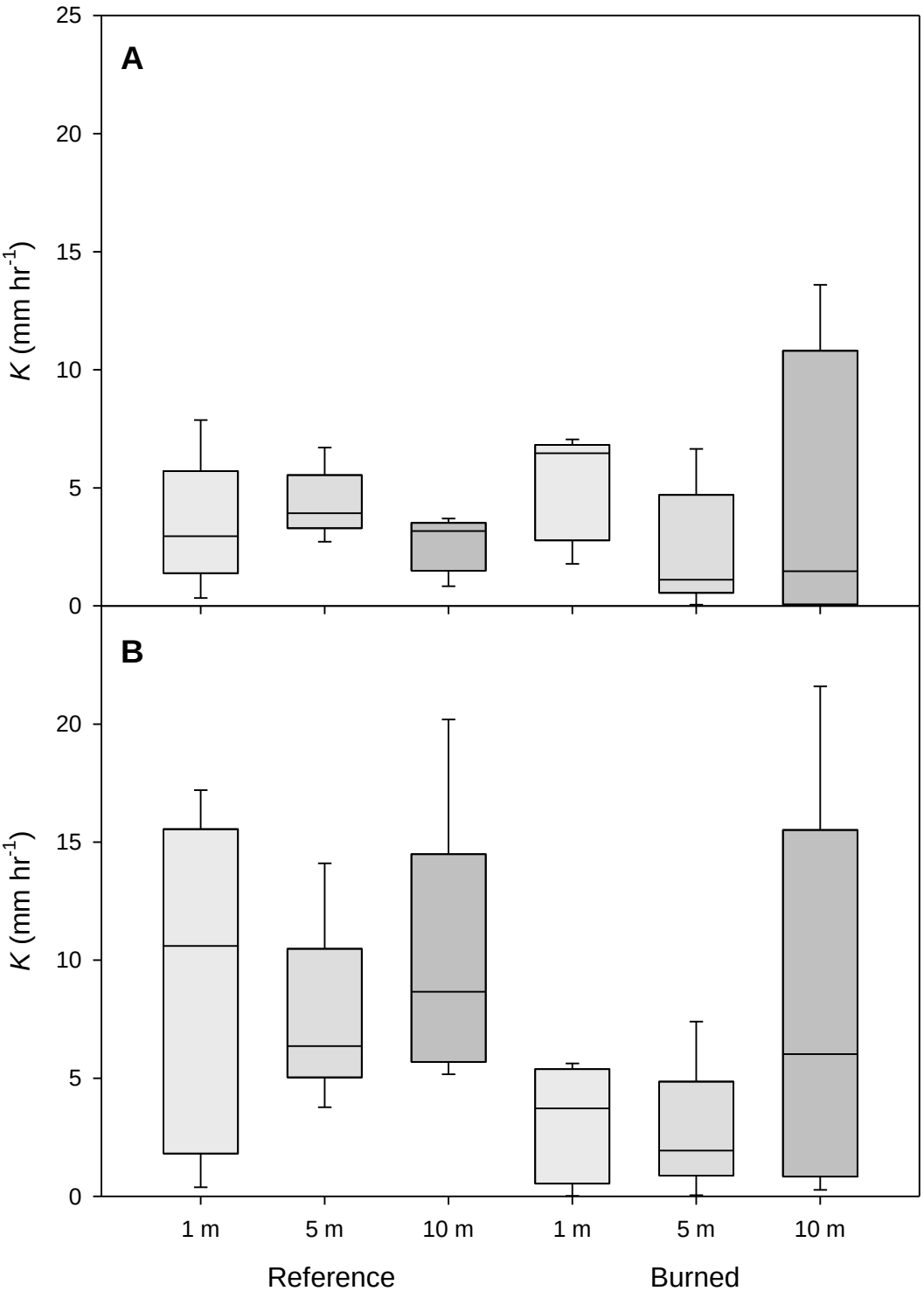

Figure 5: Unsaturated hydraulic conductivity at the A) surface of the soil layer (K_{surf}) and B) at 10 cm depth in the soil (K_{depth}) at three distances (1 m, 5 m, 10 m) from the stream edge in the reference (unburned) and burned hillslope.

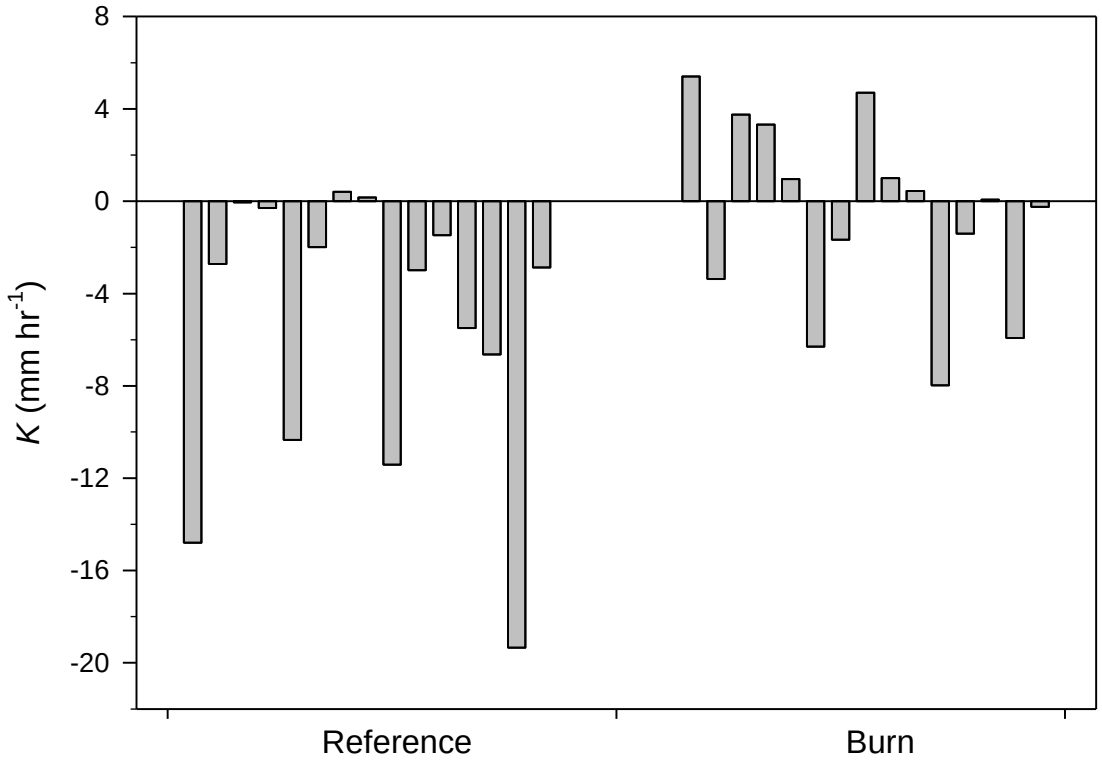

Figure 6: Difference in unsaturated hydraulic conductivity (K_{diff}) between hydraulic conductivity at the surface (K_{surf}) and at 10 cm depth (K_{depth}) for each point of measurement in the reference and the burned sites.

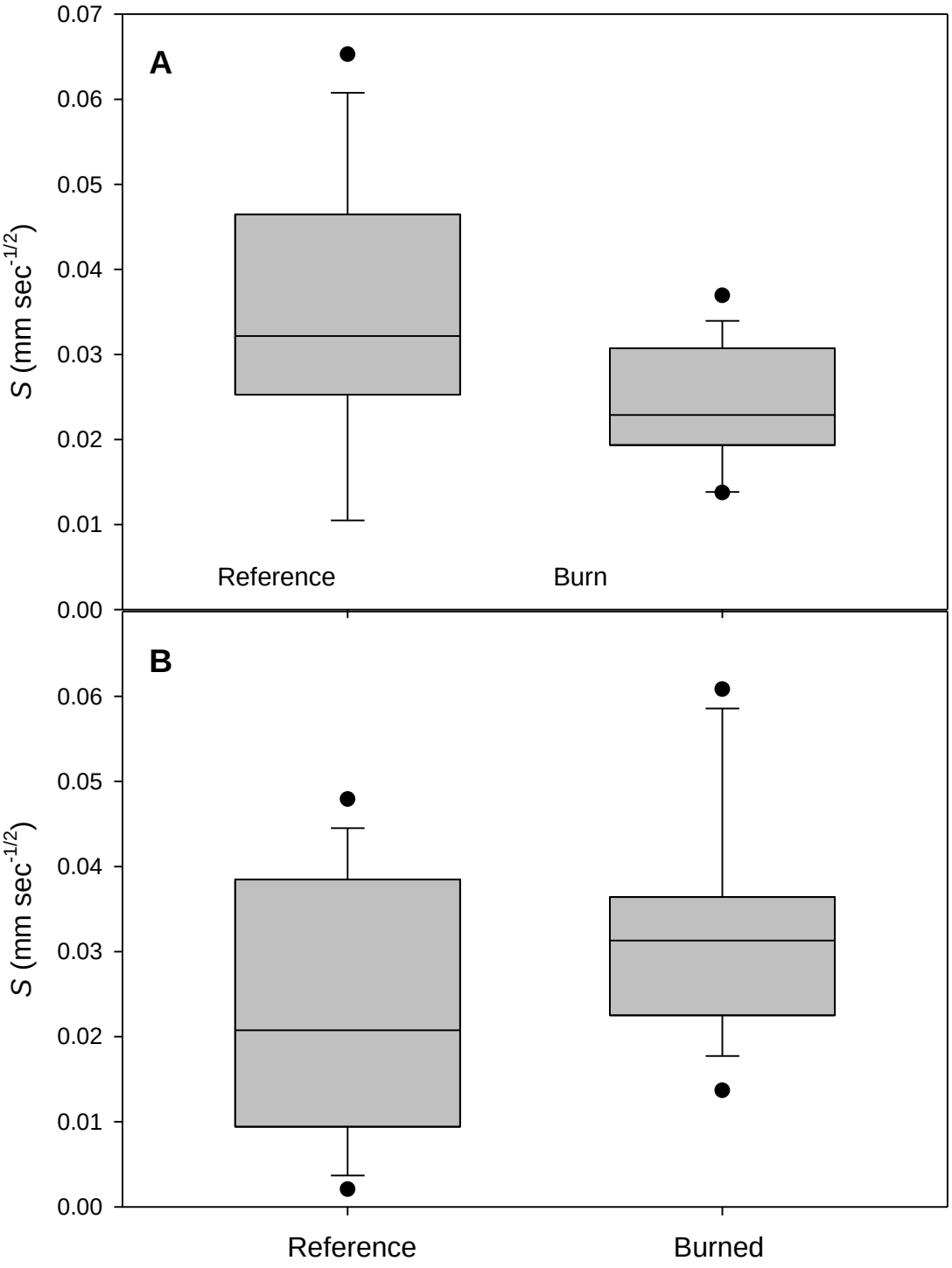

Figure 7: Sorptivity at A) the soil surface (S_{surf}) and B) at 10 cm depth in the soil (S_{depth}) for all measurement points along the reference (unburned) hillslope and on the burned hillslope.

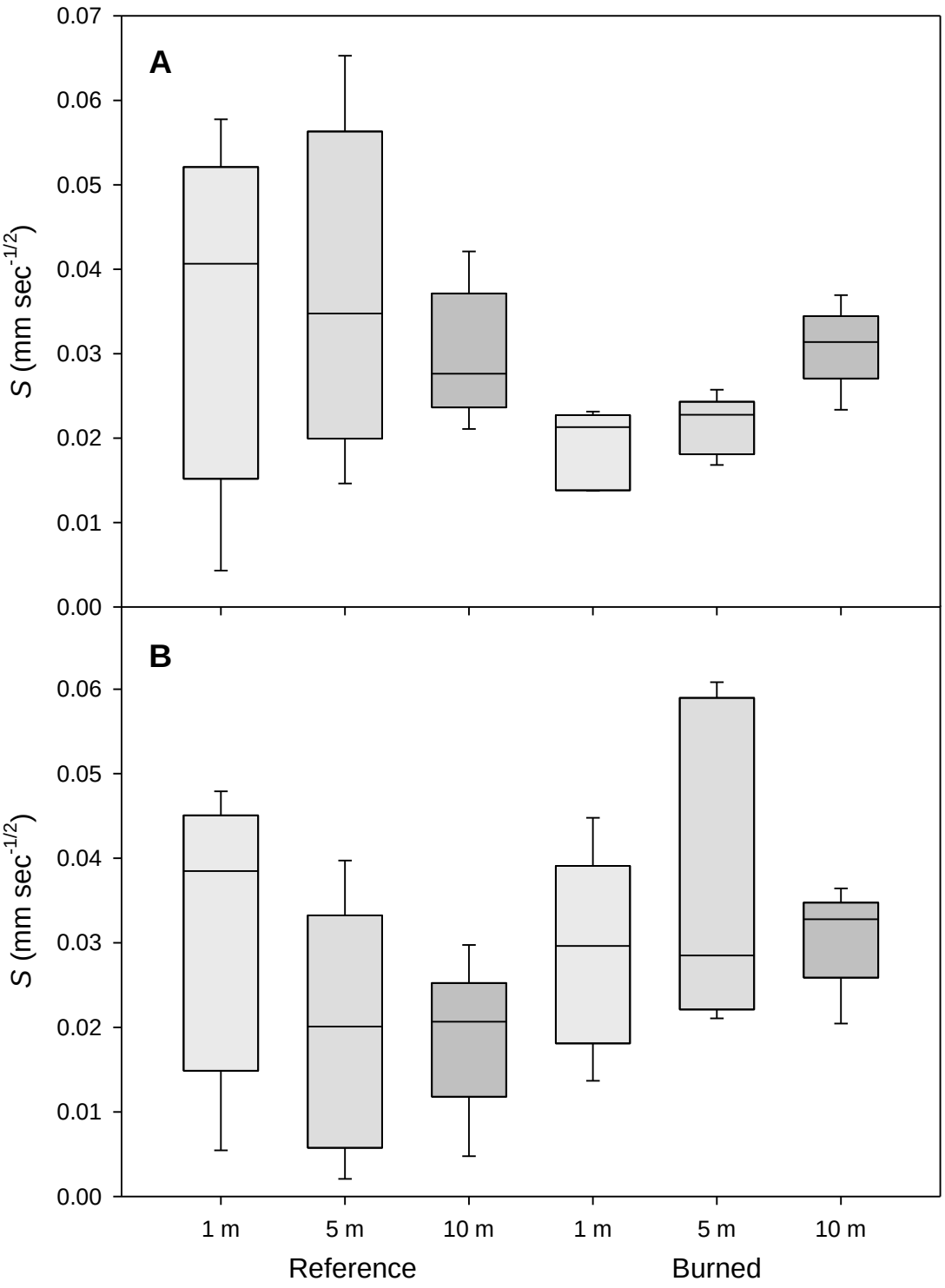

Figure 8: Sorptivity at the A) surface of the soil layer (S_{surf}) and B) at 10 cm depth in the soil (S_{depth}) at three distances (1 m, 5 m, 10 m) from the stream edge in the reference (unburned) and burned hillslope.

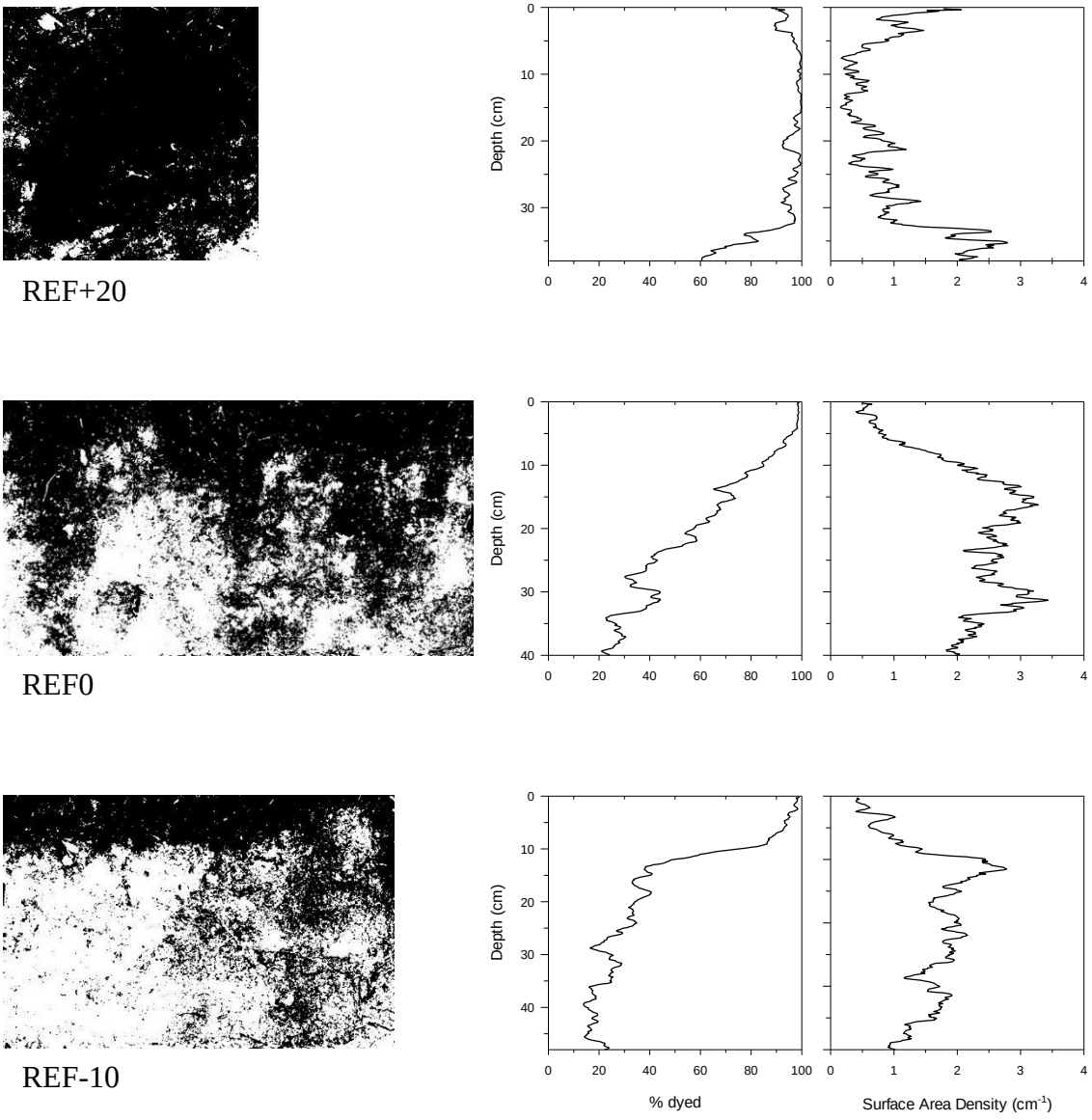

Figure 9: Processed photos (black = dye; white = no dye), volume density profiles, and surface area density profiles from the unburned, reference hillslope soil faces from a) 20 cm upslope of the bottom edge of the 1 m^2 plot (REF+20), b) at the bottom edge of the plot (REF0) and from 10 cm downslope (outside) of the 1 m^2 below (REF-10).

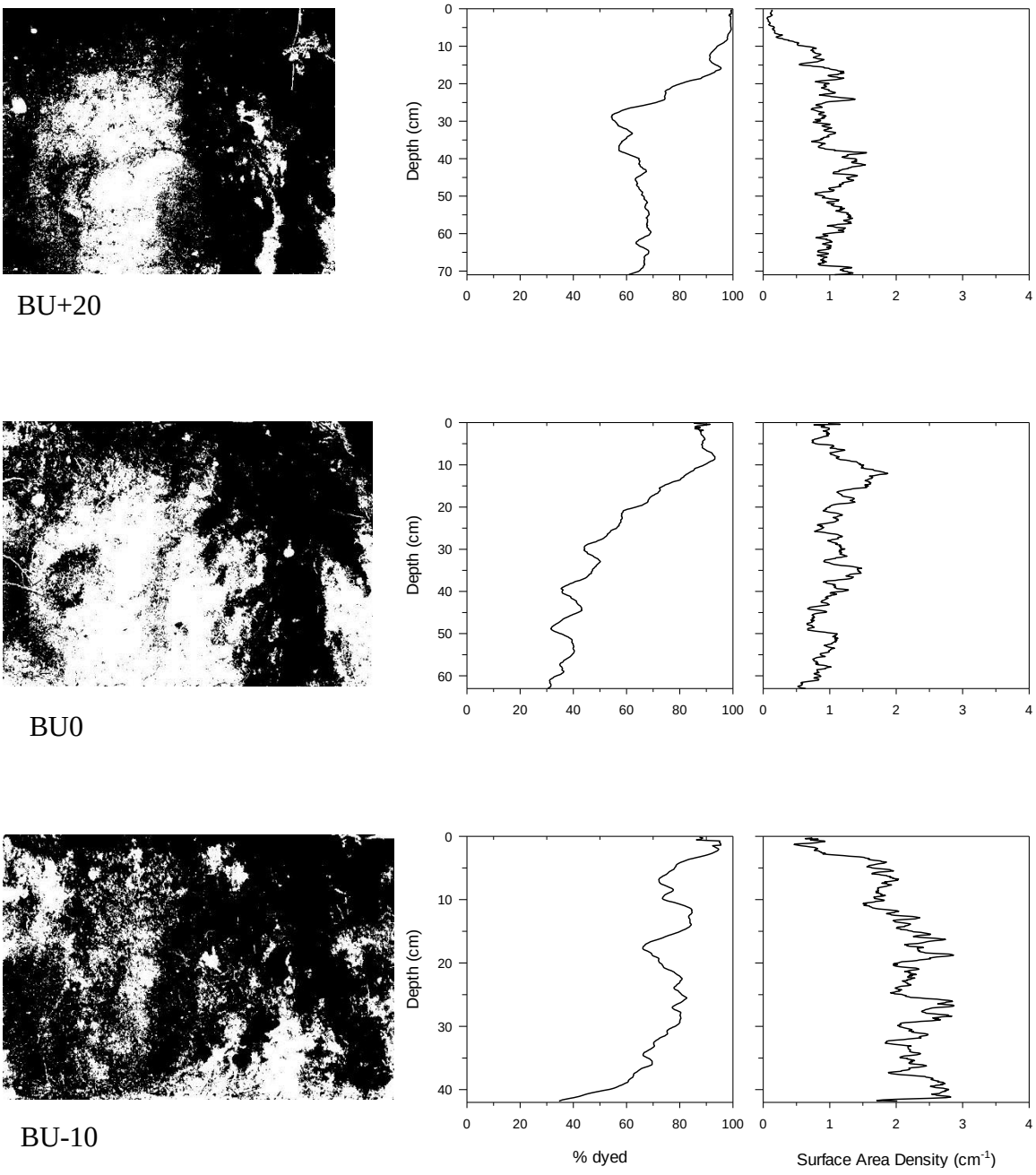

Figure 10: Processed photos (black = dye; white = no dye), volume density profiles, and surface area density profiles from burned hillslope soil faces from a) 20 cm upslope of the bottom edge of the 1 m^2 plot (BU+20), b) at the bottom edge of the plot (BU0) and from 10 cm downslope (outside) of the 1 m^2 below (BU-10).